

**FULLWAVE ANALYSIS OF MICROSTRIP IN-LINE AND OFFSET GAPS  
IN FULLY AND LATERALLY OPEN ENVIRONMENTS  
USING A DETERMINISTIC SPECTRAL DOMAIN APPROACH**

J. S. McLean, H. Ling, and T. Itoh

The University of Texas at Austin  
Department of Electrical and Computer Engineering

**ABSTRACT**

Microstrip in-line and offset gap discontinuities in both laterally open and fully open environments are, for the first time, analyzed using a deterministic spectral domain method. The analysis includes the effects of space wave and surface wave radiation and coupling in the case of fully open environments and includes the effects of *LSM* and *LSE* wave radiation and coupling in the case of laterally open environments. In the case of laterally open environments, the effect of cover height is investigated. The analysis includes the effects of two-dimensional, two-component current flow on the conductors.

**INTRODUCTION**

Microstrip in-line gap discontinuities in fully open environments have been analyzed using fullwave methods such as the spectral domain approach [1,2,3] and the space domain integral equation approach [4,5]. On the other hand, little information exists concerning the microstrip offset gap discontinuity, the geometry of which is shown in Figure 1.

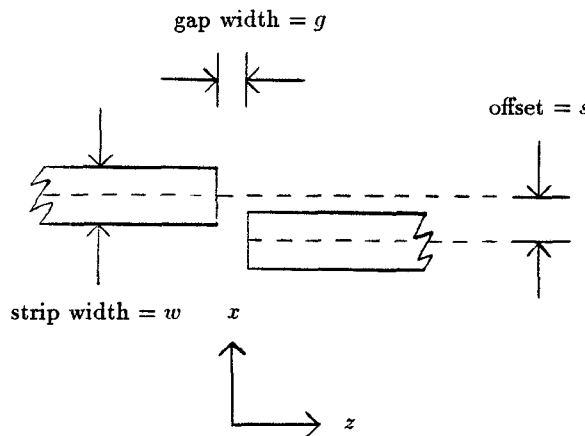


Figure 1: Geometry of Offset Microstrip Gap

Workers in the field have resorted to using an "effective" gap width in combination with an in-line gap model to estimate the capacitive coupling of the offset gap [6]. Aside from yielding only an approximate value for the coupling capacitance, this method does not account for radiation losses which are necessarily larger in the offset gap configuration. Furthermore, no analyses have been reported of gap discontinuities, whether in-line or offset, in laterally open environments. By laterally open it is meant that only a ground plane and shielding cover are present; no conducting sidewalls exist. The geometries of laterally and fully open microstrip are shown in Figures 2 and 3, respectively, for comparison. Here a deterministic spectral domain method is used to analyze microstrip in-line and offset gap discontinuities in both fully open and laterally open environments. In fully open environments, both space wave and surface wave radiation and coupling can occur, resulting in losses and spurious coupling. In laterally open environments, *LSM* (Longitudinal-Section Magnetic) and *LSE* (Longitudinal-Section Electric) mode radiation and coupling can occur. In the laterally open case, the height of the conducting cover has a significant effect on the *LSE* and *LSM* radiation. This has been noted by Jansen [7] in the analysis of radiation loss from microstrip open-end discontinuities.

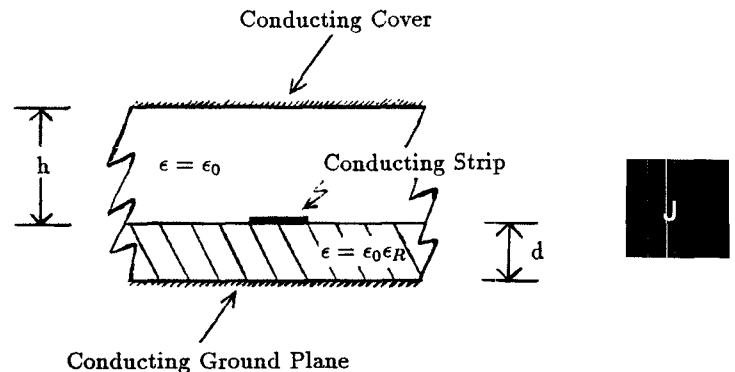


Figure 2: Laterally Open Microstrip

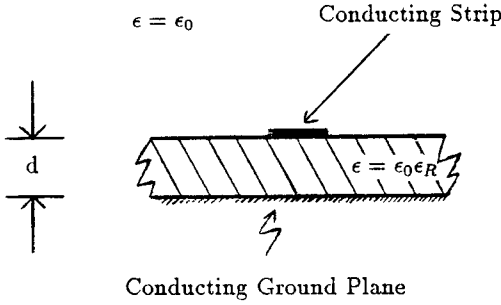


Figure 3: Fully Open Microstrip

### SUMMARY OF METHOD

The method used to analyze microstrip offset gaps is derived from that used to analyze in-line gaps which was presented in [3]. To briefly summarize, the analysis is based on a moment method which is applied to solve the Electric Field Integral Equation (EFIE) in the spectral domain. When transformed into the spectral domain the EFIE is given by:

$$\tilde{Z}_{zz}(\alpha, \beta)\tilde{J}_z(\alpha, \beta) + \tilde{Z}_{xz}(\alpha, \beta)\tilde{J}_x(\alpha, \beta) = \tilde{E}_z(\alpha, \beta) \quad (1)$$

$$\tilde{Z}_{xz}(\alpha, \beta)\tilde{J}_z(\alpha, \beta) + \tilde{Z}_{xx}(\alpha, \beta)\tilde{J}_x(\alpha, \beta) = \tilde{E}_x(\alpha, \beta) \quad (2)$$

where  $\tilde{Z}_{zz}(\alpha, \beta) \dots \tilde{Z}_{xx}(\alpha, \beta)$  are components of the spectral domain Green's function,  $\tilde{J}_z(\alpha, \beta)$  and  $\tilde{J}_x(\alpha, \beta)$  are the Fourier transforms of the current on the microstrips,  $\tilde{E}_z(\alpha, \beta)$  and  $\tilde{E}_x(\alpha, \beta)$  are the Fourier transforms of the electric field at the interface, and  $\alpha$  and  $\beta$  are the spatial Fourier transform variables. As can be seen, the EFIE takes the form of two coupled algebraic equations in the spectral domain with  $\tilde{J}_z(\alpha, \beta)$  and  $\tilde{J}_x(\alpha, \beta)$  being unknown functions. In order to apply the method of moments,  $\tilde{J}_z$  and  $\tilde{J}_x$  are expanded in terms of known functions. In order to do this efficiently, the problem is divided into three regions: a perturbed region near the offset gap discontinuity and two uniform regions on either side of the gap. In the uniform regions, the current on the microstrip is assumed to consist of only the fundamental microstrip mode of propagation. The propagation constant and transverse current distribution for the fundamental mode are determined using the conventional or eigenvalue spectral domain method. The transverse dependence of the fundamental mode current is modeled using entire domain Maxwellian functions as defined in [8]. On the excitation side, the current consists of an incident wave of known amplitude and phase and the reflected wave of unknown amplitude and phase. On the load side, the current consists of a transmitted wave of unknown amplitude and phase. In the perturbed regions, the longitudinal dependence of the current is modeled using

localized rooftop functions. The transverse dependence is modeled using entire domain Maxwellian functions. However, because of the asymmetry of the discontinuity, both even and odd functions are needed for both the transverse and the longitudinal current. Therefore, in the space domain, current on the excitation side is given by

$$\begin{aligned} J_z(x, z) = & \sum_{m=0,2,4,\dots}^M a_m J_{zm}(x - \frac{s}{2}) [e^{-j\beta_z z} - \Gamma e^{+j\beta_z z}] \\ & + \sum_{m=1}^M \sum_{n=1}^N c_{mn} J_m(x - \frac{s}{2}) \Lambda_n(z) \end{aligned} \quad (3)$$

$$\begin{aligned} J_x(x, z) = & \sum_{m=0,2,4,\dots}^M b_m J_{xm}(x - \frac{s}{2}) [e^{-j\beta_z z} + \Gamma e^{+j\beta_z z}] \\ & + \sum_{m=1}^M \sum_{n=1}^N d_{mn} J_m(x - \frac{s}{2}) \Lambda_n(z) \end{aligned} \quad (4)$$

and the current on the load side is given by

$$\begin{aligned} J_z(x, z) = & \sum_{m=0,2,4,\dots}^M a_m J_{zm}(x + \frac{s}{2}) [Te^{-j\beta_z z}] \\ & + \sum_{m=1}^M \sum_{n=1}^N e_{mn} J_m(x + \frac{s}{2}) \Lambda_n(z) \end{aligned} \quad (5)$$

$$\begin{aligned} J_x(x, z) = & \sum_{m=0,2,4,\dots}^M b_m J_{xm}(x + \frac{s}{2}) [Te^{-j\beta_z z}] \\ & + \sum_{m=1}^M \sum_{n=1}^N f_{mn} J_m(x + \frac{s}{2}) \Lambda_n(z) \end{aligned} \quad (6)$$

where  $J_{zm}(x)$  and  $J_{xm}(x)$  are the Maxwellian functions given by:

$$J_{zm}(x) = \frac{\cos(\frac{m\pi x}{w})}{\sqrt{1 - (\frac{2x}{w})^2}} \quad m = 0, 2, 4, \dots$$

$$J_{zm}(x) = \frac{\sin(\frac{m\pi x}{w})}{\sqrt{1 - (\frac{2x}{w})^2}} \quad m = 1, 3, 5, \dots$$

$$J_{xm}(x) = \frac{\cos(\frac{m\pi x}{w})}{\sqrt{1 - (\frac{2x}{w})^2}} \quad m = 1, 3, 5, \dots$$

$$J_{xm}(x) = \frac{\sin(\frac{m\pi x}{w})}{\sqrt{1 - (\frac{2x}{w})^2}} \quad m = 2, 4, 6, \dots$$

and  $\Lambda_n(z)$  are the localized rooftop functions given by

$$\Lambda_n(z) = \begin{cases} \frac{1}{h}(h - |z - z_n|) & \text{if } |z - z_n| < h \\ 0 & \text{otherwise.} \end{cases}$$

In the above expression,  $\beta_z$  is the propagation constant for the fundamental mode and  $a_0, a_2 \dots a_M$  and  $b_0, b_2 \dots b_M$  are the coefficients in the expansion of the transverse dependence of the current as determined in the eigenvalue formulation. The Fourier transforms of these expressions are substituted into the EFIE and the resultant equations are tested as in [3] to generate a square linear system which is solved for the unknowns  $c_{11} \dots c_{MN}, d_{11} \dots d_{MN}, e_{11} \dots e_{MN}, f_{11} \dots f_{MN}, \Gamma$ , and  $T$ .

## NUMERICAL RESULTS AND CONCLUSIONS

In order to compare the method with existing analysis and experimental data [5], an in-line gap in a fully open environment was analyzed. The geometry of the gap is given in Figure 4 along with the magnitude of the transmission and reflection coefficients as a function of frequency. The computed transmission and reflection coefficients agree well in both magnitude and phase (not shown) with both the theory and experiment in [5].

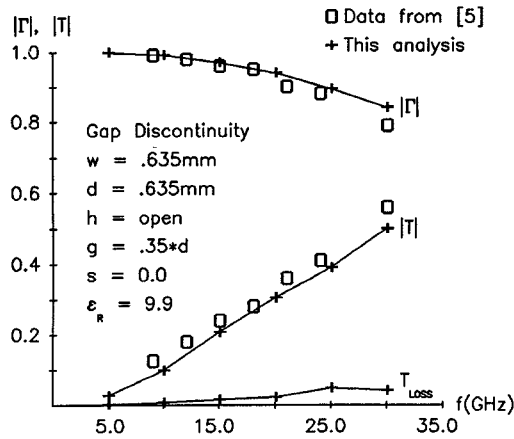


Figure 4: Open In-Line Microstrip Gap Discontinuity

The transmission loss of the discontinuity can be defined as [1]

$$T_{loss} = 1 - |\Gamma|^2 + |T|^2. \quad (7)$$

The transmission loss gives a measure of how much power is lost into surface and/or space wave radiation in the discontinuity. The transmission loss for the open in-line gap discontinuity is also plotted in Figure 4. As can be seen, the transmission loss is quite small for this structure indicating that very little power is converted from the microstrip mode into space wave radiation or the  $TM_0$  surface wave mode.

In order to analyze the effect of a shielding cover in the laterally open case, an in-line gap discontinuity with

the same geometry except for the addition of a conducting cover was also analyzed. In Figure 5, the magnitudes of the reflection and transmission coefficients for this structure are plotted as well as the transmission loss. It can be seen that that the transmission loss for the covered gap can be much higher than that of the open gap despite the absence of space wave radiation. It would seem logical to

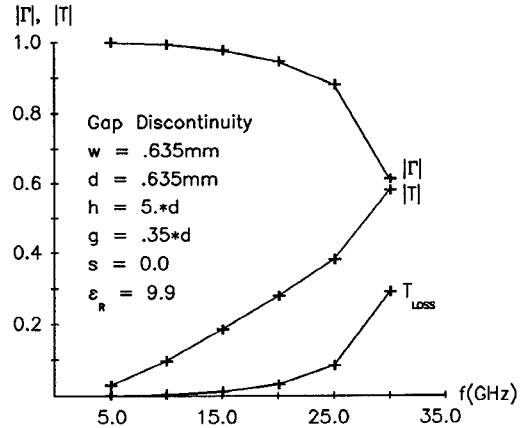


Figure 5: Covered In-Line Microstrip Gap Discontinuity

attribute this effect to the fact that the  $LSM_0$  mode for covered substrates is slower than the  $TM_0$  surface wave mode for open substrates, while the microstrip mode has essentially the same velocity whether or not the cover is present. This would cause the microstrip mode to be more apt to be converted to  $LSM_0$  mode in a covered configuration than into  $TM_0$  surface wave mode in a fully open configuration. In Figure 6, the slow-wave factors for the fundamental microstrip mode in both open and covered substrates, the  $TM_0$  surface wave mode in open substrates, and the  $LSM_0$  mode in covered substrates are plotted versus frequency.

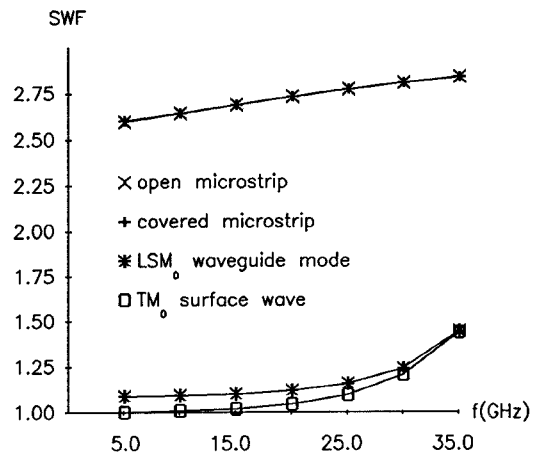


Figure 6: Slow-Wave Factors for Microstrip and Parasitic  $TM_0$  and  $LSM_0$  Modes

It can be seen that at higher frequencies the  $LSM_0$  mode is highly trapped in the substrate and hence has nearly the same velocity as the  $TM_0$  surface wave mode. Since the transmission losses of the open and covered gap discontinuities differ the most at higher frequencies, the loss must be due to a somewhat more complicated effect than that described above.

In Figure 7, the transmission and reflection coefficients and the transmission loss are given for an offset gap in an open environment. We see that while the magnitude of the transmission coefficient is much smaller than that of the in-line gap, the transmission loss is still not very significant. In Figure 8, the same gap geometry in a covered environment

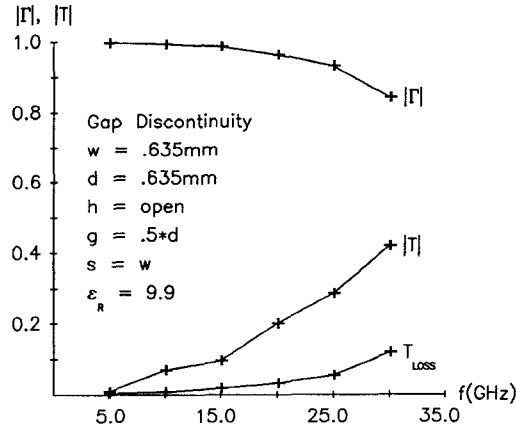


Figure 7: Open Microstrip Offset Gap Discontinuity

ment is analyzed. We see that the cover greatly exacerbates the losses incurred by the offset gap discontinuity.

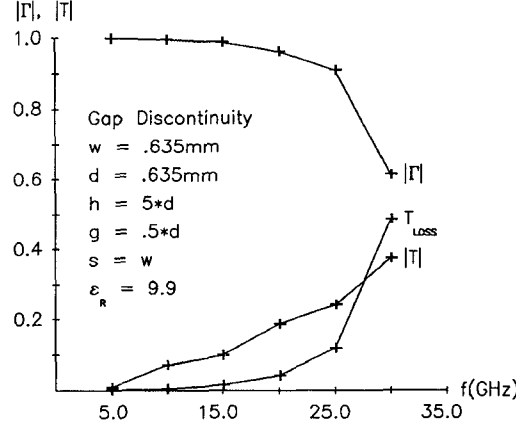


Figure 8: Covered Microstrip Offset Gap Discontinuity

In summary, in-line and offset gap discontinuities have been analyzed using a deterministic spectral domain method. It has been shown that the transmission loss is higher for offset gaps as expected. More importantly, it has been shown that a conducting cover can actually increase overall transmission loss despite preventing space wave radiation.

## BRIEF NOTE ON NUMERICAL ASPECTS

The spectral domain approach is numerically intensive as are other fullwave analyses of planar inhomogeneous structures. However, because the bulk of the numerical work involves quadrature, the method is quite amenable to vectorization. This work was performed on a Convex C-220 computer. Typical run times are about 15 minutes per data point with 64 subsectional basis functions. However, due to a lack of development time, the vector capabilities of the machine were not fully exploited.

## REFERENCES

- [1] R. W. Jackson and D. M. Pozar, "Full-Wave Analysis of Microstrip Open End and Gap Discontinuities," *IEEE Trans. Microwave Theory Tech.*, vol. MTT-33, no. 10, Oct. 1985, pp. 1036-1041.
- [2] H. Yang, N. G. Alexopoulos and D. R. Jackson, "Microstrip Open-End and Gap Discontinuities in a Substrate-Superstrate Structure," *IEEE Trans. Microwave Theory Tech.*, vol. MTT-37, No. 10, Oct. 1989, pp. 1542-1546.
- [3] J. S. McLean, H. Ling, and T. Itoh, "Spectral Domain Analysis of Microstrip Gaps and Gap-Coupled Resonators," *Proc. 20th European Microwave Conf.*, Sept. 10-13, 1990, Budapest.
- [4] P.B. Katehi and N. G. Alexopoulos, "Frequency-dependent Characteristics of Microstrip Discontinuities in Millimeter-Wave Integrated Circuits," *IEEE Trans. Microwave Theory Tech.*, vol. MTT-33, no. 10, Oct. 1985, pp. 1029-1035.
- [5] M. Drissi, F. Hanna, and J. Citerne, "Theoretical and Experimental Investigations of Open Microstrip Gap Discontinuities," *Proc. 18th European Microwave Conf.*, Sept. 12-16, 1988, Stockholm, Sweden.
- [6] C. Chang and T. Itoh, "Microwave Active Filters Based on Coupled Negative Resistance Method," *The University of Texas Microwave Laboratory Report No. 90-P-3*, The University of Texas at Austin, Austin Texas April 1990.
- [7] J. Boukamp and R. H. Jansen, "The High Frequency Behavior of Microstrip Open-Ends in Microwave Integrated Circuits Including Energy Leakage," *Proc. 14th European Microwave Conf.*, Sept. 10-13, 1984, Liege, Belgium, pp. 142-147.
- [8] T. Itoh, *Numerical Techniques for Microwave and Millimeter-wave Passive Structures*, John Wiley and Sons, New York, 1989.